HYDROTHERMAL SYNTHESIS OF FLOWER-SHAPED ZnSNANOCRYSTALS FOR NONENZYMATIC ELECTROCHEMICAL GLUCOSE DETECTION

Y.ZHENG[a], Z.WANG[a], B.DENG[b],F.HAN[a], F.PENG[a], Y. PEN[c], L.HE[d], L.FU[a*]
[a]*Institute of Botany, Jiangsu Province and Chinese Academy of Sciences, Nanjing Botanical Garden, Mem. Sun Yat-Sen, Nanjing, China*
[b]*JiangsuJunma Park Technology Co. Ltd, Jiangsu, China*
[c]*College of Forestry and Biotechnology, Zhejiang Agriculture and Forestry University, Lin'an, Zhejiang, China*
[d]*Beijing Petrochemical Engineering Corp. LTD, Chaoyang District Tianjuyuan Building No. 7, Beijing, China*

In this letter, we reported a hydrothermal method for synthesizing flower-shaped ZnSnanocrystal using $Zn(NO_3)_2 \cdot 6H_2O$ and thioacetamide as precursors. The prepared flower-shaped ZnS was characterized by SEM, XRD, EDX and fluorescence spectrophotometer. The results indicate the proposed synthesis method could yield a high purity of flower-shaped ZnS with diameters of 110 nm.The application of these ZnSnanoflowersas electrochemical glucose sensor was successfully explored. Due to the high surface area and excellent electrocatalytic activity of the ZnSnanoflower, the constructed electrochemical sensor exhibited a high selectivity and a low detection limit. Moreover, the proposed glucose sensor also displayed excellent stability, reproducibility and anti-interference property.

(Received December 14, 2015; Accepted February 18, 2015)

Keyword: ZnS; Hydrothermal; Electrocatalysis; Sensor; Glucose

1. Introduction

Zinc sulfide (ZnS) is group II–IV binary compound semiconductor and it has traditionally shown exceptional physical and chemical properties and a promise for novel diverse applications, such as electroluminescence, sensors, lasers, and so on[1-4].Its structure and chemical properties are comparable to ZnO, but the ZnS have not been investigated in much detail relative to ZnO[5-10].

Reliable and fast detection of glucose is important in many fields such as clinical diagnostics and food industry[11-20]. Moreover, blood glucose monitoring is particularly important in the care of diabetes because it affecting about 200 million people around the world [21, 22]. Therefore, the development of glucose sensors with high sensitivity and selectivity, good stability, fast response, and low cost has driven tremendous research efforts for the past decade. Particularly, electrochemical glucose sensor plays a leading role in this field. However, the most of the glucose electrochemical biosensors are based on glucose oxidase bound to electrode transducers. The disadvantages of the enzymatic sensors are lack of stability because of the intrinsic nature of the enzyme. The performance of the enzyme can be easily influenced by chemical compounds, pH, temperature and humidity [23].Therefore, the development of a nonenzymatic glucose sensor is an alternative approach and it exhibits attractive advantages including sufficient stability, simplicity of operation and oxygen limitation-free [24, 25].In this work, we reported the fabrication of a nonenzymatic glucose sensor based onflower-shaped ZnSnanocrystals modified grassy carbon electrode. The fabricated sensor exhibits a wide linear

*Corresponding author: lifugyt@gmail.com

detection range with a low detection limit.Moreover, the sensor also exhibits high selectivity to the target analyte.

2. Experimental

2.1 Materials

Zinc nitrate hexahydrate ($Zn(NO_3)_2 \cdot 6H_2O$), thioglycolic acid (TGA), thioacetamide (TAA), glucose, uric acid (UA), dopamine (DA), ascorbic acid (AA) and acetylcholine (Ach) were purchased from Sigma-Aldrich. All other chemicals used were analytical grade reagents without further purification. Milli-Q water (18.2 MΩ cm) was used throughout the experiments.

2.2 Preparation of flower-shaped ZnS nanocrystals

In a typical preparation process, as-received zinc nitrate hexahydrate (5 g) was dissolved in 50 mL of distilled water. Then, 1 mL of TGA (0.05 M) was slowly added into the solution. After 10 min stirring, a stoichiometric amount ofTAA was slowly added as S source. After 30 min stirring, the solution was transferred to a 100 mL Teflon-lined stainless steel autoclave and heated at 110—150°C for 5 h.The obtained samples were centrifuged and dried in an oven at 70°C to result ZnS(denoted as ZnS-1, ZnS-2 andZnS-3 for the hydrothermal temperature of 110, 130 and 150°C, respectively).

2.3 Characterizations

X-ray diffraction patterns were collected from 20° to 90° in 2θ by a XRD with Cu Kα radiation (D8-Advanced, Bruker, Germany). Surface morphology of samples were analyzed by scanning electron microscope (SEM, S-4700, HITACHI, Japan). The photoluminescence (PL) emission curves were obtained by a fluorescence spectrophotometer. The excitation of all analysis was set at 280 nm at room temperature and the emission curves were recorded from 300 to 500 nm.

2.4 Fabrication of glucose electrochemical sensor and electrochemical measurement

For the fabrication of glucose electrochemical sensor, the as-synthesized ZnSnanoflowers were coated onto the glassy carbon electrode (GCE). The GCE was carefully polished using alumina slurry (1.0, 0.3, and 0.05 mm in sequence) followed by rinsing with water. For the electrode surface modification, 5 μL of ZnS suspension was cast onto the surface of the pretreated GCE and dried at room temperature.Electrochemical measurements were performed on a CH Instruments 660A electrochemical Workstation (CHI-660 A, CH Instruments, Texas, USA) using a three electrode system. A platinum wire was used as the auxiliary electrode and an Ag/AgCl (3M KCl) as the reference electrode.

3. Results and discussion

Fig. 1 shows the typical SEM images of ZnS-1 and ZnS-3. It can be observed that the ZnSnanocyrstals formed through the hydrothermal condition display a flower like nanostructure. The average diameter of the ZnSnanoflower is about 110 nm (calculated based on more than 200 ZnSnanoflowers). It also can be seen that the morphology of the ZnS flowers formed under 110°C and 150°C showed no significant difference, indicating our proposed synthesis method is reliable and has excellent robustness.

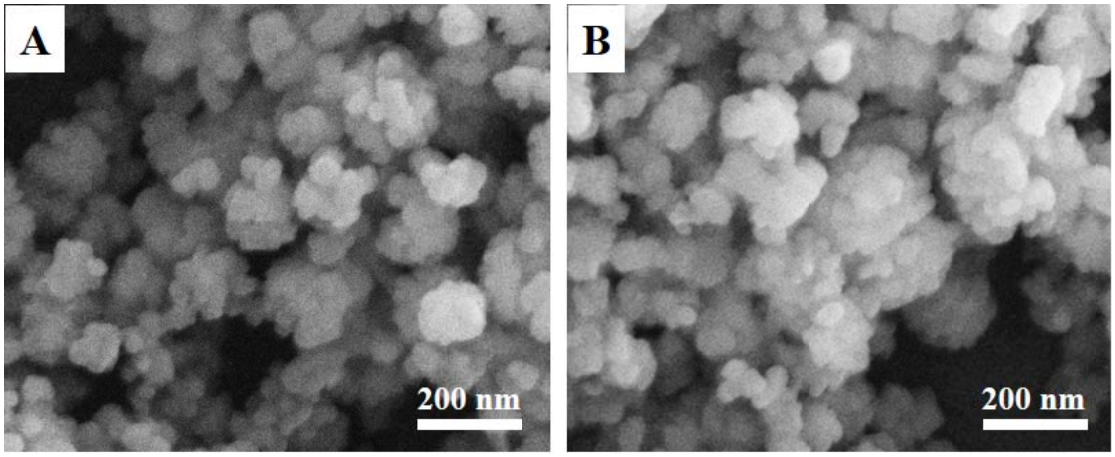

Fig. 1. SEM images of (A) ZnS-1 and (B) ZnS-3.

The elemental information of the as-prepared ZnSnanoflowers was analyzed by EDX. Figure 2A displays the EDX spectrum of ZnS-3. As shown in the figure, the EDX spectrum of the ZnS-3 displays the only existence of Zn and S. Therefore, our proposed hydrothermal method could successfullyproduce ZnSnanoflowers with high purity.

Figure 2B demonstrates the powder X-ray diffraction patterns of ZnS-1, ZnS-2 and ZnS-3.All of the samples exhibited the peaks at 28.8°, 33.1°, 47.3°, 56.8°, 59.1°, 69.7°, 77.8°, 79.2° and 88.9°, corresponding to the (111), (200), (220), (311), (222), (400), (331), (420) and (422) phases of cubic zinc blende (sphalerite) (JCPDS No.05-0566). Moreover, no diffraction peaks detected from the impurity phases such as TGA, S, ZnO, further indicate the proposed method could produce pure cubic sphaleriteZnSnanoflowers. Table 1 presents the crystallite size of ZnSnanoflowers prepared via different hydrothermal temperatures according to Scherrer's equation[26, 27]. Results suggest that the crystallite size of the ZnSnanoflowers was slowly increasing along with the hydrothermal temperature increasing.

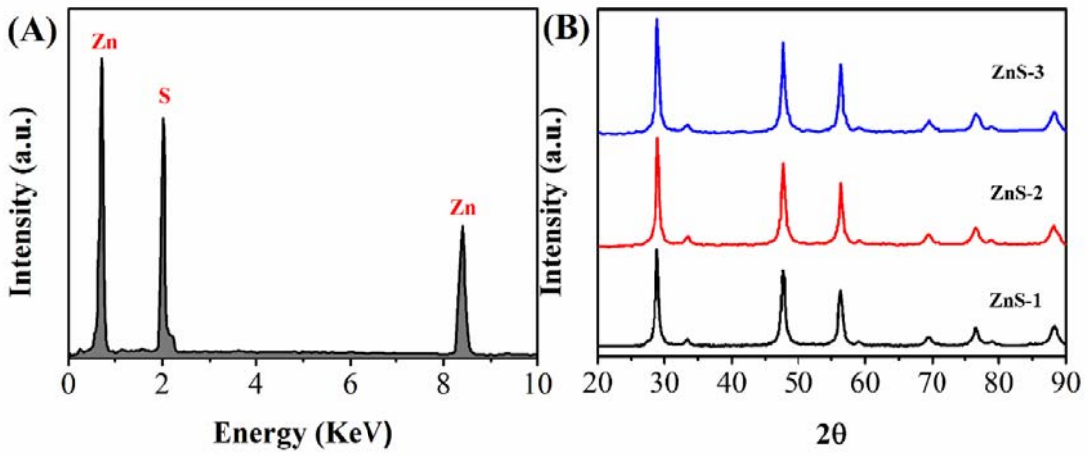

Fig. 2: (A) EDX spectrum of ZnS-3. (B) XRD patterns ofZnS-1, ZnS-2 and ZnS-3.

Table 1: The crystallite size of the ZnS-1, ZnS-2 and ZnS-3.

Temperatures (°C)	Full width at half of maximum (111)	Crystallite size (nm)
110	0.3135	27.3
130	0.3002	27.5
150	0.2892	28.3

The luminescence property of synthesized ZnS was also investigated. Figure 3 shows the room temperature photoluminescence spectrum of free ZnS-3 at the excitation wavelength of 280 nm.The near band edge emission of ZnSnanoflowers occurs at about 330 nm is attributed to the recombination of the photogenerated electron hole pairs. The visible emission band at 380 nm and some other minor peaks is mainly due to the recombination of electrons caused by surface defects and vacancies [28].

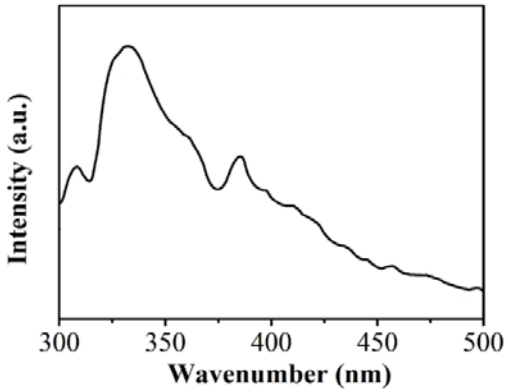

Fig. 3.PL spectrum of ZnS-3

The electrochemical behavior of 1 mM glucose was investigated by cyclic voltammetry at bare GCE, ZnS-1/GCE, ZnS-2/GCE and ZnS-3/GCE respectively. Figure 4 presents the CV profiles of GCE, ZnS-1/GCE, ZnS-2/GCE andZnS-3/GCEin the absence and presence of 1 mM glucosein 0.1M PBS. It can be seen that the bare GCE only exhibited a small background current. In contrast, ZnSnanoflowers modified GCEs all displayed significant enhancement toward oxidation of glucose. Among the electrode, ZnS-3/GCE showed the best performance for electro-oxidation of glucose. A well-defined oxidation peak was observed at 0.57 V with current of 87.01 μA. This enhancement of glucose detection can be ascribed to the excellent electrocatalytic activity of ZnSnanoflowers and their specific nanostructure, which owing a high specific surface area.

The effect of pH on the electro-oxidation of glucose has been investigated. Figure 5A shows the oxidation peak current of glucose at various pH value of PBS. It can be seen that the peak currents gradually increase along with the pH increases from 4 to 7.5. The maximum value was obtained at pH 7.5 with 87.01 μA. Afterwards, the current responses decrease when further increasing of the pH. The effect of amount of ZnS-3 on the electrochemical detection performance of the glucose was also studied. As shown in Figure 5B, the oxidation peak current exhibits obvious increase tendency along with the amount of modifier increases from 1 to 5 μL. However, further increasing ZnS leads a slightly decreasing of the oxidation current response. The reason of current decreasing probably due to the electrons of glucose take longer time to transfer through relatively thicker layer of ZnS.

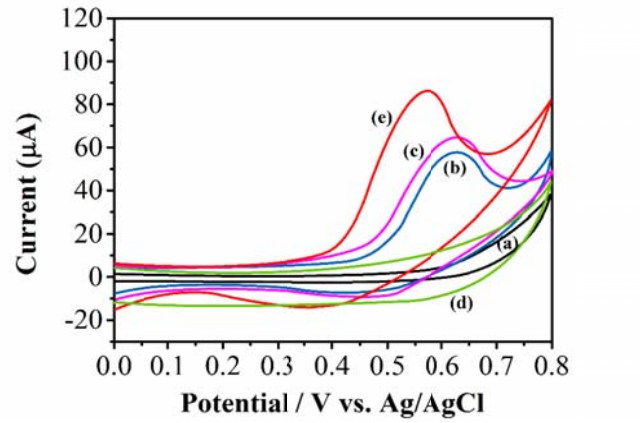

Fig.4. Cyclic voltammograms of (a) bare GCE, (b) ZnS-1/GCE and (c) ZnS-2/GCE in the presence of 1 mM glucose. (d, e) ZnS-3/GCE in 0.1 M PBS in the absence or presence of 1 mM glucose. Scan rate: 50 mV/s

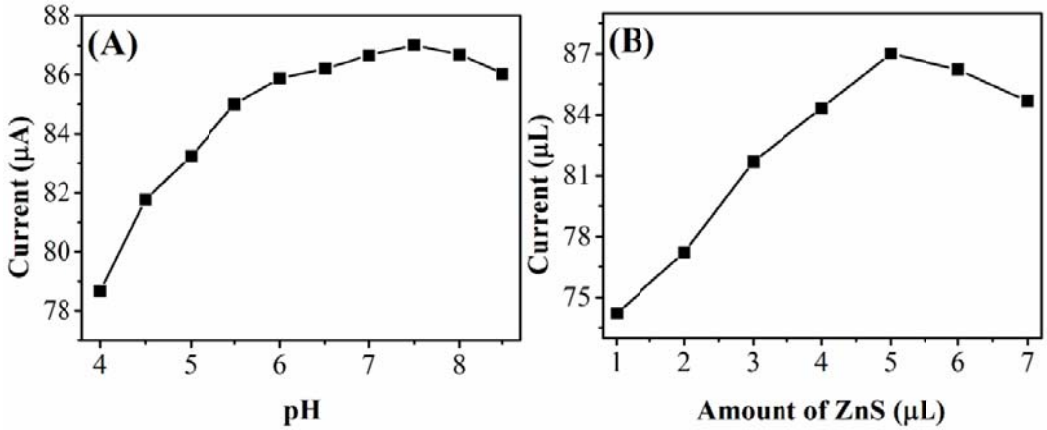

Fig. 5.The plot of I_{pa} versus (A) pH of PBS (B) amount of modifier for glucose determination

Fig 6A shows the typical amperometric response of the ZnS-3/GCE for the successive addition of glucose from 0.1 μM to 1500 μM at the applied potential of 0.57 V. It can be observed from figure that the electrode shows a clear increase in current response after successive additions of glucose. It also can be seen that the response current increased rapidly after each addition of glucose, and returned to the steady-state within 5 s, suggesting the fast response of the ZnS-3/GCE to glucose.Figure 6B displays linear current response for glucose within the concentration range of 0.1 μM to 1500 μM. The corresponding regression equation can be expressed as: $I = 0.08509C + 1.97476$ (where $I$is in μA and C is in μM; $R_2 = 0.9988$). The detection limit was calculated to be 0.071 μM ($S/N = 3$).

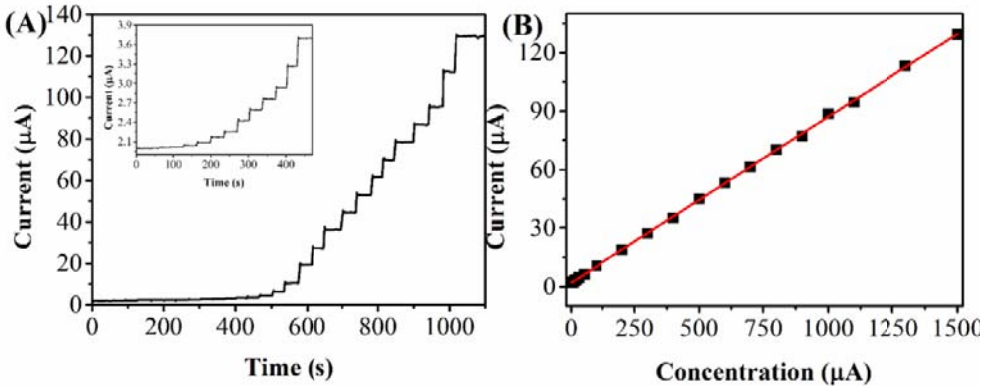

Fig. 6.(A) Amperometric response of the ZnS-3/GCE with successive additions of glucose into PBS. Measured at 0.57 V. Inset: Magnification of current responds from 1 to 20 μM. (B)Plot of current responses versus glucose concentrations in the range of 0.1 to 1500 μM.

The selectivity of the proposed sensor was also investigated because the major challenge in nonenzymatic glucose determination is to eliminate the influence of interfering species. In this case, the influence of some physiological interferents has been investigated. Figure 7 shows the typical amperometric response of ZnS-3/GCE upon the addition of glucose (1 mM), AA (5 mM), DA (5 mM), UA (5 mM) and Ach (5 mM). Results indicate that no obviously change in the current response after addition of 5 mM AA, DA, UA and Ach. Therefore, the proposed sensor is highly selective towards the detection of glucose.

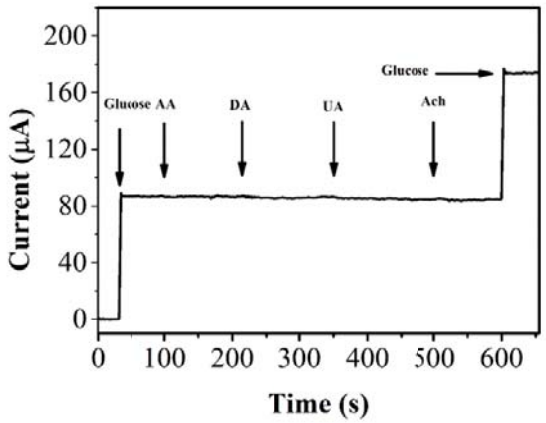

Fig. 7.Amperometric current response of ZnS-3/GCE to the addition of 1 mM glucose, 5 mM AA, 5 mM DA, 5 mM UA and 5 mM Ach into continuously stirred 0.1 M PBS at the operating potential of 0.57 V.

The reproducibility and stability of the proposed glucose sensor were evaluated as well. Eight fresh prepared ZnS-3/GCE were used for determining 1 mM glucose. The relative standard deviation (RSD) was calculated to be 3.11% with a mean current response of 86.98 μA.Stability of the proposed glucose sensor was tested by 25 successive measurements in PBS containing 1 mM glucose. The results only showed a 3.3 % decrease of stability compared with the original test,which is stable enough for use as an electrochemical sensor of glucose.

4. Conclusion

In conclusion, we demonstrated the hydrothermal method for synthesizing flower-shaped ZnS nanocrystal.The ZnS modified GCE has been successfully utilized in the selective determination of glucose.In comparison to bare GCE, the ZnS modified GCE exhibited a superiorhigherelectrocatalytic activity towards oxidation of glucose.The proposed glucose sensor also exhibited a wide detection range with fast response and a lower detection limit. Moreover, the sensor displayed an excellent anti-interference property and stability.

Reference

[1] N. Soltani, A. Dehzangi, A. Kharazmi, E. Saion, W.M.M. Yunus, B.Y. Majlis, M.R. Zare, E. Gharibshahi, N. Khalilzadeh, Chalcogenide Letters **11,** 79 (2014).
[2] P.A. Luque, A.S. Villasenor, M.A. Quevedo-Lopez, A. Olivas, Chalcogenide Letters **11,** 105 (2014).
[3] F. Haque, K.S. Rahman, M.A. Islam, M.J. Rashid, M. Akhtaruzzaman, M.M. Alam, Z.A. Alothman, K. Sopian, N. Amin, Chalcogenide Letters **11,** 189 (2014).
[4] M.M. Byranvand, A.N. Kharat, Journal of Ovonic Research **10,** 191 (2014).
[5] X. Fang, T. Zhai, U.K. Gautam, L. Li, L. Wu, Y. Bando, D. Golberg, Progress in Materials Science **56,** 175 (2011).
[6] L. Fu, A. Wang, Y. Zheng, W. Cai, Z. Fu, Materials Letters **142,** 119 (2015).
[7] L. Fu, Z. Fu, Ceram Int **41,** 2492 (2015).
[8] L. Fu, W. Cai, A. Wang, Y. Zheng, Materials Letters **142,** 201 (2015).
[9] M.A. Ciolan, I. Motrescu, D. Luca, M. Nagatsu, Digest Journal of Nanomaterials and Biostructures **9,** 483 (2014).
[10] P. Muthukumar, T.M. Selvakumari, C. Rangasami, S. Ganesan, Digest Journal of Nanomaterials and Biostructures **8,** 1455 (2013).
[11] J. Pulit, M. Banach, Digest Journal of Nanomaterials and Biostructures **8,** 787 (2013).
[12] A.J. Jegadeesan, L. Karunamoorhty, N. Arunkumar, Materials and Manufacturing Processes **30,** 155 (2014).
[13] J.H. Kim, S.-A. Jun, Y. Kwon, S. Ha, B.-I. Sang, J. Kim, Bioelectrochemistry **101,** 114 (2015).
[14] Z. Zhu, C. Chen, X. Zhu, R. Xie, A.J. Flewitt, W.I. Milne, Journal of Nanoscience and Nanotechnology **15,** 3196 (2015).
[15] H.-T. Lu, X.-H. Cao, Z.-J. Yang, S. Chen, Y. Fan, Analytical Letters **48,** 137 (2014).
[16] T. Juřík, P. Skládal, Detection of hydrogen peroxide and glucose by enzyme product precipitation on sensor surface, Chemical Papers, 2015, pp. 167.
[17] X. Qin, Q. Li, A. Asiri, A. Al-Youbi, X. Sun, Gold Bull **47,** 3 (2014).
[18] O. Olarte, K. Barbé, W. Van Moer, Y. Van Ingelgem, A. Hubin, Biomedical Signal Processing and Control **14,** 9 (2014).
[19] S. Das, M. Saha, Journal of Pharmaceutical Analysis **4,** 351 (2014).
[20] M. Moumene, A. Tabet-Aoul, M. Gougis, D. Rochefort, M. Mohamedi, International Journal of Electrochemical Science **9,** 176 (2014).
[21] G.-h. Wu, X.-h. Song, Y.-f. Wu, X.-m. Chen, F. Luo, X. Chen, Talanta **105,** 379 (2013).
[22] F. Scarlat, A. Scarisoreanu, N. Verga, F.I. Scarlat, C. Vancea, Journal of Intense Pulsed Lasers and Applications in Advanced Physics **4,** 55 (2014).
[23] R. Wilson, A.P.F. Turner, Biosensors and Bioelectronics **7,** 165 (1992).
[24] X. Niu, M. Lan, C. Chen, H. Zhao, Talanta **99,** 1062 (2012).
[25] C.J. Chirayil, L. Mathew, S. Thomas, Reviews on Advanced Materials Science **37,** 20 (2014).
[26] Y. Xia, P. Yang, Y. Sun, Y. Wu, B. Mayers, B. Gates, Y. Yin, F. Kim, H. Yan, Adv. Mater. **15,** 353 (2003).
[27] H. Zhang, R. Xie, T. Sekiguchi, X. Ma, D. Yang, Mater Res Bull **42,** 1286 (2007).
[28] S. Wageh, Z.S. Ling, X. Xu-Rong, Journal of Crystal Growth **255,** 332 (2003).